Effects of Distal Point-Site Mutations on the Binding and Catalysis of Dihydrofolate Reductase from *Escherichia coli*†

Joseph Adams, Kenneth Johnson, Robert Matthews, and Stephen J. Benkovic*
Department of Chemistry, 152 Davey Laboratory, The Pennsylvania State University, University Park, Pennsylvania 16802
Received February 6, 1989; Revised Manuscript Received April 25, 1989

ABSTRACT: The importance of salt bridge interactions at the NADPH binding site of dihydrofolate reductase has been studied by using site-directed mutagenesis. The mutations R44L and H45Q respectively disrupt the ionic contacts made between the 2′-phosphate and pyrophosphoryl moiety of the coenzyme and the N-terminal region of helix C. Equilibrium fluorescence experiments indicate that while the overall binding of NADPH to both free mutants is weakened by 1.1 and 1.5 kcal/mol (H45Q and R44L, respectively), the binding of dihydrofolate and tetrahydrofolate is unaffected. Despite the similar binding energies for both mutants, the transition state for the chemical hydride step is differentially destabilized relative to wild type (0.6 and 1.8 kcal/mol for H45Q and R44L, respectively). Both stopped-flow and pre-steady-state experiments suggest that the root of this effect may lie in multiple conformations for the E–NADPH complex of R44L. The ability of both mutants to transmit their effects beyond the local environment of the NADPH pocket is manifested in several details: (1) the pK_a of Asp-27 (25 Å away from the sites of mutation) is elevated from 6.5 in the wild type to 7.5 and 8.4 in H45Q and R44L, respectively; (2) NADPH elevates the off rates for tetrahydrofolate from 12 s^{-1} in the wild type to >45 s^{-1} in R44L; and (3) bound tetrahydrofolate decreases the affinity of the enzymes for NADPH as reflected in the K_m from 2 to 40 μM for H45Q (similar to wild type) but from 8 to 5000 μM for R44L.

Dihydrofolate reductase (DHFR)[1] (5,6,7,8-tetrahydrofolate:$NADP^+$ oxidoreductase) catalyzes the NADPH-dependent reduction of 7,8-dihydrofolate (H_2F) to 5,6,7,8-tetrahydrofolate (H_4F). Further derivatization of tetrahydrofolate provides a number of coenzymes involved in one carbon transfer reactions including those important in the biosynthesis of purines and thymidylate. Consequently, DHFR has become a vital target for a host of "antifolate" compounds that not only are potent inhibitors of DNA biosynthesis but also show adequate specificity for DHFR's from diverse sources. For example, trimethoprim (TMP) functions as an antibactericide, pyrimethamine as an antifungicide, and methotrexate (MTX) as an anticancer agent.

X-ray crystallographic data on the DHFR–MTX binary complex from *Escherichia coli* have elucidated the fine details of the folate binding pocket (Matthews et al., 1977). By analogy with MTX, H_2F binds deep in the active site with pteridine and benzoyl rings making hydrophobic interactions with a number of key residues (e.g., Leu-54, Ile-50, and Phe-31). Asp-27 is the only ionizable amino acid in the active-site interior and forms a strong salt bridge with the N-1 of MTX. Although no crystal structure presently exists for the *E. coli* DHFR with NADPH bound, the E–NADPH–MTX ternary complex of the *Lactobacillus casei* DHFR has been solved. Due to the high degree of backbone homology between the two enzymes, NADPH can be simulated in the *E. coli* pocket (Filman et al., 1982). The coenzyme binds in an extended conformation with the nicotinamide ring closely positioned to the pterin ring at the folate site by hydrophobic residues (e.g., Ile-5, Ala-14, and Ile-94) and the 2′-phosphate and pyrophosphoryl moiety anchored by strong ionic contacts (Arg-44 and His-45).

The elucidation of the wild-type kinetic scheme has revealed a wealth of information concerning ligand ordering, proton donation, and hydride transfer (Stone & Morrison, 1982; Howell et al., 1986; Fierke et al., 1987). One particularly interesting feature of this mechanism is the increase in the dissociation rate of tetrahydrofolate in the presence of NADPH. Although this coenzyme/product synergism is critical in defining the rate-determining step under steady-state conditions at low pH, a clear physical description of this effect is unavailable to date. In an effort to evaluate this phenomenon as well as coenzyme conformational changes and catalytic effects, two point-site mutants of DHFR have been studied. Both changes, R44L and H45Q, disrupt ionic contacts made between the 2′-phosphate and pyrophosphoryl moiety of NADPH and the guanidine and imidazole side chains of R44 and H45, respectively. The primary goal of this work is to establish a role for specific ionic interactions far from the reaction center of the folate cavity.

Materials and Methods

Materials. 7,8-Dihydrofolate (H_2F) was prepared by the dithionite reduction of folic acid (Blakley, 1960), and (6*S*)-tetrahydrofolate was prepared from H_2F by enzymatic conversion with DHFR (Matthews & Huennekens, 1960). Purification of H_4F was achieved on a DE-54 resin with a linear triethylammonium bicarbonate gradient (Curthoys et al., 1972). NADPH, $NADP^+$, MTX, and folic acid were purchased from Sigma.

2,4-Diamino-6,7-dimethylpteridine (DAM) was purchased from ICN Pharmaceuticals. [4′(*R*)-^{2}H]NADPH (NADPD) and TNADPH (thionicotinamide adenine dinucleotide phosphate, reduced) were prepared (Stone & Morrison, 1982) by using *Leuconostic mesenteroides* alcohol dehydrogenase

† This work was supported by NIH Grant GM24129 and NSF Grant PCM-81-04495.

[1] Abbreviations: DHFR, dihydrofolate reductase; H_2F, dihydrofolate; fol, folic acid; H_4F, tetrahydrofolate; NADPH, nicotinamide adenine dinucleotide phosphate, reduced; $NADP^+$, nicotinamide adenine dinucleotide phosphate; TNADPH, thionicotinamide adenine dinucleotide phosphate, reduced; MTX, methotrexate; R44L, Arg-44 → Leu; H45Q, His-45 → Gln.

0006-2960/89/0428-6611$01.50/0

purchased from Research Plus, Inc., and purified by the method of Viola et al. (1979). Excess NaCl was removed from the purified NADPD by a Biogel P-2 desalting column (Howell et al., 1987). Ligand concentrations were determined spectrophotometrically by using the following extinction coefficients: H_4F, 28 000 M^{-1} at 297 nm, pH 7.5 (Kallen & Jencks, 1966); H_2F, 28 000 M^{-1} at 282 nm, pH 7.4 (Dawson et al., 1969); folic acid, 27 600 M^{-1} at 282 nm, pH 7.0 (Rabinowitz, 1960); MTX, 22 100 M^{-1} at 302 nm in 0.1 N KOH (Seeger et al., 1949); NADPH, 6200 M^{-1} at 339 nm, pH 7.0; TNADPH, 11 300 M^{-1} at 395 nm; $NADP^+$, 18 000 M^{-1} at 259 nm, pH 7.0 (P-L Biochemicals, 1961). The concentrations of H_2F and NADPH were also checked by turnover with DHFR. The H45Q and R44L mutants were constructed, respectively, by Jin-Tan Chen and Cinda Herndon as previously described (Chen et al., 1985; Perry et al., 1987). All kinetic measurements were obtained at 25 °C in a buffer which contained 50 mM 2-(*N*-morpholino)ethanesulfonic acid, 25 mM tris(hydroxymethyl)aminomethane, 25 mM ethanolamine, and 100 mM sodium chloride (MTEN buffer). The buffers were purged with argon when H_4F was used.

Steady-State Kinetics. Initial velocities for the enzyme reactions were measured by using either a Cary 219 UV-visible spectrophotometer or the stopped-flow instrument (absorbance mode). The molar absorbance change used in the former case was 11 800 M^{-1} (Stone & Morrison, 1982) and 3000 M^{-1} in the latter case. The stopped-flow apparatus was used to measure steady-state turnover only when very high NADPH concentrations were needed (>200 μM). DHFR was preincubated with varying amounts of NADPH before H_2F was added to remove hysteretic effects (Penner & Frieden, 1985). The observed dissociation constants for DAM inhibition were determined by plotting $1/v$ vs [DAM] (Segel, 1975; Stone & Morrison, 1982).

Stopped-Flow Experiments. Transient binding and pre-steady-state kinetics were performed on a stopped-flow apparatus designed and built in the laboratory of Johnson (1986). The instrument has a 1.6-ms dead time and a 2-mm sample cell and can be used in either a transmittance or a fluorescence mode. Interference filters (Corion Corp.) were used for emission output and a monochromator for excitation input. Typically, ligand binding experiments were monitored by using a selected excitation wavelength of 290 nm and an output filter of 340 nm. To measure coenzyme fluorescence, an output filter of 450 nm was used. Absorbance measurements were made by converting the transmittance at 340 nm. A molar absorbance change for the enzyme reaction of 3000 M^{-1} was determined at 340 nm. In most cases, an average of 6–10 traces was taken at a given set of conditions for data analysis.

Following a trigger impulse, data were collected by a computer over a selected time range. Kinetic data were fit by using a nonlinear least-squares computer program that analyzed the transients as a single or double exponential or a single exponential followed by a linear rate (Dyson & Isenberg, 1971; Johnson, 1986). Binding and pre-steady-state data were then transferred to a Vax microcomputer and fit to more complicated mechanisms by using the kinetic simulation program KINSIM (Barshop & Frieden, 1983).

Fluorescence Titrations. The thermodynamic dissociation constants (K_d) of ligands and DHFR were measured by fluorescence titration. In this experiment, the quenching of the intrinsic enzyme fluorescence at 340 nm upon excitation at 290 nm was monitored as a function of ligand concentration (Birdsall et al., 1980; Stone & Morrison, 1982; Taira & Benkovic, 1988). In separate control experiments, a known quantity of tryptophan was titrated to correct for the inner filter absorbance effects of the added ligand. Typically, the enzyme concentration used was either at or slightly less than the K_d of the ligand. The data were fit to a nonlinear least-squares fitting program previously described (Taira & Benkovic, 1988).

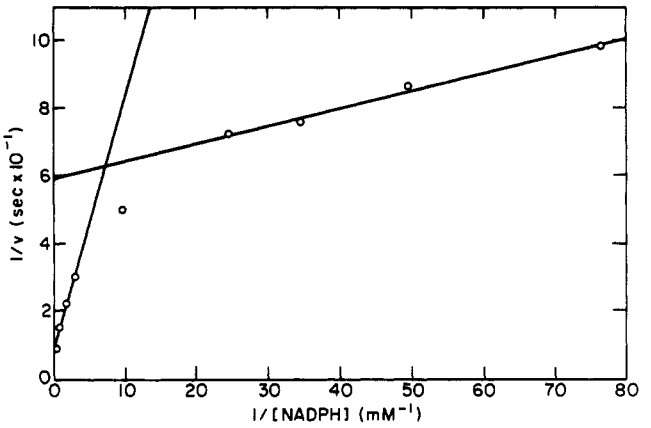

FIGURE 1: Variation of the initial velocity (v) of the enzyme reaction with varying concentrations of NADPH (12–3000 μM) for R44L. H_2F concentration was fixed at 50 μM, pH 7.0, 25 °C.

Table I: Steady-State Kinetic Parameters for R44L and H45Q

	mutants		
	R44L	H45Q	WT
$V1$ (s^{-1})	1.7 ± 0.1	1.9 ± 0.2	
$K1$ (μM)	8.3 ± 0.9	4.0 ± 0.5	
p$K_a(V1)$	>9.5	>9.5	
$V2$ (s^{-1})	27 ± 4	7.6 ± 0.2	12[a]
$K2$ (μM)	5000 ± 1000	40 ± 2	5[b]
p$K_a(V2)$	8.5 ± 0.04	8.9 ± 0.05	8.4[a]

[a] Parameters were determined at 100 μM NADPH and varying [H_2F] (Fierke et al., 1987). [b] Parameter was determined at 10 μM H_2F and varying [NADPH] at pH 7.0 (Fierke et al., 1987).

RESULTS

Steady-State Parameters: pH Dependence. The steady-state parameters V and K_m have been determined for wild type at fixed [NADPH] and varied [H_2F] as well as at fixed [H_2F] and varied [NADPH] (Fierke et al., 1987; Stone & Morrison, 1982, 1984). In both cases, double-reciprocal plots are virtually linear over all concentrations of substrate and coenzyme. For both mutants, however, these plots show significant curvature under conditions of fixed [H_2F] (50 μM). An example of this negative deviation is illustrated in Figure 1. Since two distinct V's and K_m's are approached, the following modified form of the Michaelis–Menten equation (eq 1) was used to

$$v = V1[S]/(K1 + [S]) + V2[S]/(K2 + [S]) \quad (1)$$

analyze all steady-state data. In this equation, [S] is the substrate concentration, v is the initial reaction velocity, and $V1$ and $K1$ are, respectively, the maximal velocity and the apparent dissociation constant approached at low NADPH while $V2$ and $K2$ are those approached at high NADPH. $V1$, $V2$, $K1$, and $K2$ for R44L and H45Q were obtained by using this analysis. These results at pH 7 are shown in Table I. For both mutants, increasing the fixed level of H_2F (30–100 μM) had no effect on the observed curvature of these lines, indicating that substrate is sufficiently saturating.

The V vs pH profile for wild type is controlled by an acidic residue at the active site (Asp-27) that ionizes with an observed pK_a of 8.4. Previous studies have shown that the shape of this profile is due to the change in the rate-limiting step from

Table II: Thermodynamic Dissociation Constants for Ligands to Mutant and Wild-Type DHFR

ligand	K_d (μM)		
	R44L	H45Q	WT
NADPH	3.5 ± 0.2	2.0 ± 0.2[a]	0.33[b]
$NADP^+$	130 ± 22		22[b]
NADH	4.3 ± 0.2		5.8 ± 0.6
H_2F	0.26 ± 0.02	0.33 ± 0.05[a]	0.22[b]
H_4F		0.07 ± 0.02[a]	0.07[b]

[a] K. Taira and S. J. Benkovic, personal communication. [b] Fierke et al. (1987).

Scheme I

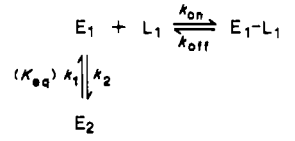

pH-independent H_4F dissociation at low pH to hydride transfer at high pH (Fierke et al., 1987). The net effect is an attenuation of V above pH 8.4 due to the pH-dependent chemical step. The results of the steady-state experiments are shown in Table I. Although there is no detectable dependence in $V1$ for both mutants up to pH 9.5, pK_a's of 8.5 and 8.9 in $V2$ are obtained for R44L and H45Q, respectively.

Steady-State Isotope Effect on V. Since product dissociation is rate limiting at low pH and hydride transfer at high pH, a full kinetic isotope effect of 3 on V using [4′(*R*)-^{2}H]-NADPH (NADPD) is seen only at high pH for wild type (Stone & Morrison, 1984; Howell et al., 1986; Chen et al., 1987; Fierke et al., 1987). Steady-state isotope experiments on $V1$ and $V2$ were performed for R44L and H45Q. For R44L, no isotope effect on $V1$ is seen at either low or high pH although one is seen on $V2$ at low pH (2.0 ± 0.5). For H45Q, a full isotope effect is seen on $V2$ at high pH (2.9 ± 0.2), but virtually none is seen on $V1$ or $V2$ at low pH.

Thermodynamic Dissociation Constants. The thermodynamic binding of ligands to DHFR can be analyzed by following the quenching of the intrinsic enzyme fluorescence upon ligand titration (Birdsall et al., 1980; Stone & Morrison, 1984). Computer fitting of the fluorescence quenching data corrected for inner filter absorbance effects yields the overall thermodynamic dissociation constant (K_d) for the desired ligand to the enzyme. Table II shows the K_d's of various ligands to both free mutant and wild-type enzymes. Although the binding of H_2F and H_4F is unaffected, clearly an effect is seen for NADPH. For both mutants, the overall binding of NADPH is equivalently weakened by 1.1 kcal/mol for H45Q and 1.5 kcal/mol for R44L. The binding of NADH (a poor ligand for DHFR) to R44L is, however, very similar to wild type. All K_d values show no pH dependence between 6 and 9 (data not shown).

Kinetic Binding of Ligands: Relaxation Experiments. The binding of ligands to DHFR can be monitored by following the time-dependent quenching of the intrinsic enzyme fluorescence at 340 nm upon stopped-flow mixing of the ligand with enzyme (Dunn et al., 1978; Dunn & King, 1980; Cayley et al., 1981). Cayley et al. (1981) have concluded that the enzyme equally exists in two slowly interconverting forms, E_1 and E_2, of which only one binds ligand, E_1. This mechanism is illustrated in Scheme I and gives rise to a rapid ligand-dependent phase and slower ligand-independent phase upon mixing.

For pseudo-first-order reaction conditions ([L] ≫ [E]), the observed rate constant (k_{obs}) for binding L_1 to E_1 can be approximated by $k_{obs} = k_{on}[L] + k_{off}$ where k_{on} and k_{off} are the association and dissociation rate constants, respectively. A plot of k_{obs} vs [L] yields k_{on} from the slope and k_{off} from the intercept. For this scheme, the rate constant for enzyme interconversion (k_1) is determined from the slow phase rate and the equilibrium constant ($K_{eq} = k_1/k_2$) from the ratio of the relative amplitudes of the fast and slow phases. For wild-type DHFR, k_1 is 0.03 s^{-1}, and K_{eq} is 1. The association and dissociation rate constants for several ligands to both mutants are listed in Table III. Consistent with the K_d measurements, k_{on} and k_{off} for H_2F and H_4F are close to those of wild type. However, for NADPH, k_{on} is decreased and k_{off} is elevated for both mutants. This parallels the larger K_d's for NADPH to H45Q and H44L.

Table III: Association and Dissociation Rate Constants of Ligands to Mutants and Wild-Type Enzymes

ligand	DHFR	k_{on} (μM^{-1} s^{-1})	k_{off} (s^{-1})
H_2F	WT[a]	42	47
	H45Q		
	R44L	34 ± 4	50 ± 3
H_4F	WT[a]	24	<1
	H45Q	16 ± 2	1.5 ± 0.4
	R44L	14 ± 3	1.7 ± 0.5
NADPH	WT[a]	20	3.5
	H45Q	8.0 ± 0.2	10 ± 4
	R44L	1.0 ± 0.1	30 ± 5

[a] Fierke et al. (1987).

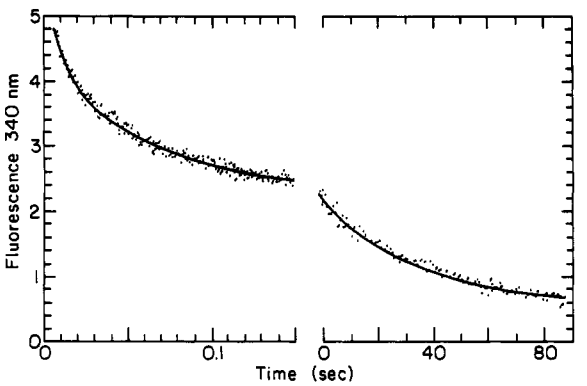

FIGURE 2: Time-dependent fluorescence quenching of the intrinsic enzyme fluorescence upon mixing 0.15 μM wild-type DHFR and 1.0 μM NADPH at pH 7.0, 25 °C. The binding trace was sampled over two time ranges by collecting 250 data points over 0.15 s and 250 points over 90 s.

To verify the mechanism outlined in Scheme I for NADPH binding to wild-type enzyme, stopped-flow experiments were done over a large range of NADPH concentrations, 0.5–50 μM. If NADPH exclusively binds E_1, then the ligand-dependent portion of the binding trace should have single-exponential character at all coenzyme concentrations. Figure 2 shows the time-dependent fluorescence quenching of wild-type DHFR at 1.0 μM NADPH over two time frames, 0.15 and 90 s. The first frame is composed of two fast phases (75 ± 5 and 24 ± 2 s^{-1}) which are well separated from the slower interconversion phase (0.032 ± 0.002 s^{-1}). These studies have collectively shown that the rapid binding traces are only monophasic over a limited concentration range (2–10 μM). Above or below this range, a second ligand-dependent phase emerges. We have interpreted these findings as representing NADPH binding to two separate enzyme conformers, namely, E_1 and E_2. Control experiments done with freshly purified NADPH confirmed that the additional phases were not due to an impurity in the commercial sample. A plot of k_{obs} vs [NADPH] is shown in Figure 3. Line A corresponds to

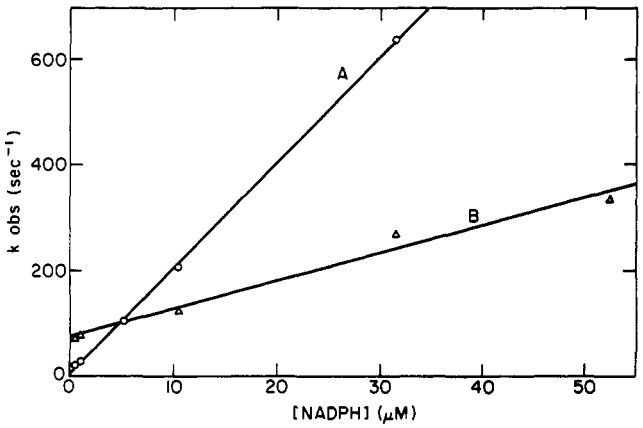

FIGURE 3: Variation of k_{obs} for the two rapid stopped-flow transients with varying NADPH concentrations for wild type DHFR. Line A (○) corresponds to E_1 binding while line B (△) corresponds to E_2 binding.

Scheme II

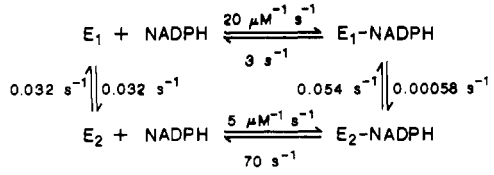

coenzyme binding to E_1 (k_{on} = 20 ± 0.2 μM^{-1} s^{-1}, k_{off} = 3 ± 0.3 s^{-1}) and is consistent with previous binding data (Fierke et al., 1987). Line B, which was derived from the emergence of the second phase, represents coenzyme binding to E_2 (k_{on} = 5 ± 0.4 μM^{-1} s^{-1}, k_{off} = 70 ± 3 s^{-1}). Thus, NADPH binding is precisely described in three kinetic phases rather than two. This phenomenon has been hitherto kinetically invisible due to the constrained working concentrations of NADPH. Nevertheless, comparison of both on and off rates for the wild-type enzyme indicates that E_1 binds NADPH approximately 100-fold tighter than does E_2 (k_{off}/k_{on} for E_1 = 0.15 μM, k_{off}/k_{on} for E_2 = 14 μM) so that at equilibrium approximately 99% of the bound coenzyme is in the E_1–NADPH binary form. Furthermore, at high concentrations the coenzyme can bind sufficient E_2 so that the interconverting species is E_2–NADPH → E_1–NADPH rather than E_2 → E_1. The rate coefficient associated with the third phase increases from 0.032 s^{-1} (E_2 → E_1) to 0.054 s^{-1} (E_2–NADPH → E_1–NADPH). The reverse rate constant for the latter isomerization can then be determined by considering the binding as a thermodynamic cycle. The combined data shown in Scheme II describes the complete kinetic mechanism for NADPH binding to wild-type DHFR.

Kinetic Dissociation Constants: Competition Experiments. The dissociation rate constants of ligands to DHFR can be measured by using a competition experiment (Dunn et al., 1978). For this technique, the enzyme–ligand complex (E–L_1) is preequilibrated before a large excess of a competing ligand (L_2) is rapidly mixed. If there is a sufficient difference in the fluorescence signal between E–L_1 and E–L_2, then an exponential rate is observed. This process is described in Scheme III.

Scheme III

$$E\text{–}L_1 \underset{k_{-1}}{\overset{k_1}{\rightleftharpoons}} E + L_1$$

$$E + L_2 \underset{k_{-2}}{\overset{k_2}{\rightleftharpoons}} E\text{–}L_2$$

Table IV: Dissociation Rate Constants for Ligands to Mutant and Wild-Type Enzymes

ligand	enzyme species	trapping ligand	k_{off} (s^{-1}) R44L	H45Q	WT[a]
H_2F	E–H_2F	MTX	21 ± 5		22
H_2F	E-TNH–H_2F	MTX	10 ± 2		43
H_4F	E–H_4F	MTX	1.6 ± 0.2	1.6 ± 0.2	1.4
H_4F	E-NH–H_4F	MTX	1.8 ± 0.3[b]	7.6 ± 0.8	12.5
NADPH	E-NADPH	$NADP^+$	46 ± 7	25 ± 10	3.6
NADPH	E-NH-fol	$NADP^+$	22 ± 6		
$NADP^+$	E–$NADP^+$	NADPH	300 ± 50	300 ± 30	290

[a] Fierke et al. (1987). [b] Not at saturating [NADPH]. Calculated as 70 s^{-1}; see Results.

When $k_1(L) \ll k_2(L) \gg k_{-1}$, the observed exponential (k_{obs}) is equal to the dissociation rate constant for L_1 (k_{-1}). The above is valid if k_{obs} is independent of the concentration of L_2. The off rates for a number of ligands to binary and ternary complexes of the mutants were determined by using this experiment. These results along with those of wild type are shown in Table IV.

The values of H_2F and H_4F for the binary complexes of both mutants are close to the dissociation rate constants for wild type although those for NADPH are different. This again is consistent with the unaffected binding of folate derivatives and the weakened binding of NADPH to the free mutants relative to wild type. The off rates determined by relaxation (Table III) and competition (Table IV) techniques are either identical or differ by approximately a factor of 2. We consider these discrepancies, if any, to be within experimental error of both methods. Neither H_2F nor NADPH dissociation is accelerated by the coenzyme or substrate analogues TNADPH or folic acid.

Pre-Steady-State Kinetics. The hydride transfer rate (k_{hyd}) for wild type has been isolated by using pre-steady-state fluorescence energy transfer experiments (Fierke et al., 1987). In this technique, the protein emission spectra excites the nicotinamide portion of NADPH at 340 nm which in turn emits at 450 nm. Since the oxidized nicotinamide of NADP displays no emission in this spectral region, the consumption of NADPH as well as any protein or coenzyme conformation changes that alter the fluorophore environment in the first turnover can be monitored.

The observed k_{hyd} for both mutants was determined by using stopped-flow fluorescence energy transfer. In this experiment, enzyme is preequilibrated with NADPH before H_2F is rapidly mixed. For H45Q, the pre-steady-state transient at pH 7 is composed of a single-exponential burst (k_{hyd} = 340 ± 20 s^{-1}) followed by linear steady-state turnover (7.5 s^{-1}). The burst was confirmed to be hydride transfer since repeating the experiment with NADPD gave a full isotope effect of 3 ± 0.2 (data not shown). In contrast, the traces for R44L clearly show two distinct phases before the linear steady-state rate. An example of this at pH 7 is shown in Figure 4. Under these conditions, the first phase corresponds to a rate of 370 ± 30 s^{-1} and the second to 45 ± 3 s^{-1}. Upon repeating the experiment with NADPD, a full isotope effect of 3 ± 0.3 was obtained for the slower second phase while virtually no isotope effect (1.3 ± 0.3) was obtained for the first phase. In addition, the biphasic nature of this effect is not removed by preequilibration with H_2F (data not shown). Since both coenzyme and substrate concentrations used were sufficiently high to dispell the fast phase as due to ligand association, the nature of this step was assumed to be conformational.

All pre-steady-state transients were fit to the kinetic simulation program KINSIM (Barshop & Freiden, 1983) using

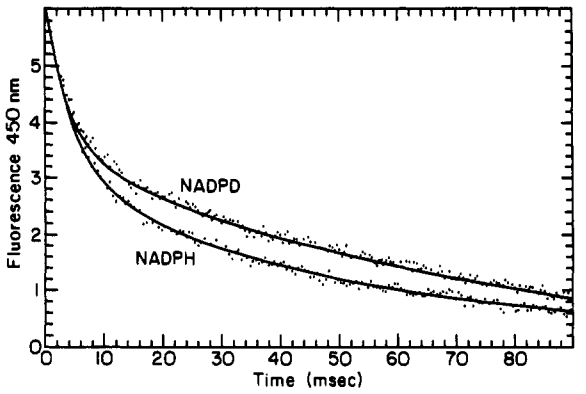

FIGURE 4: Measurement of the pre-steady-state burst for R44L by stopped-flow fluorescence energy transfer. DHFR is preincubated with either NADPH or [4'(*R*)-^{2}H]NADPD, and the reaction is initiated with H_2F. Final conditions are 10 μM R44L, 100 μM NADPH(D), 150 μM H_2F, pH 7.0, 25 °C. The lines drawn through both transients are KINSIM computer fits to Scheme V.

either Scheme IV or Scheme V. Both mechanisms involve rapid H_2F binding (k_1), hydride transfer (k_2), and dissociation of NADP (k_3) and H_4F (k_4) (note: NADPH binding, which is included in k_4, is diffusion controlled and can be kinetically ignored). Scheme V differs from Scheme IV since it involves the conformation step, k_c. Consequently, all data for H45Q were fit to Scheme IV while data for R44L were fit to Scheme V. Values for k_1, k_{-1}, k_3, and k_4 used for all simulations were taken from Tables III and IV. Since H_2F and NADPH concentrations are high, k_{-4} can be ignored due to rapid trapping of the product complex, E·H_4F. In addition, the reverse rate of hydride transfer (k_{-2}) is small for wild type (0.6 s^{-1}) so that it is insignificant compared to k_2. Experiments designed to determine k_{-2} (Fierke et al., 1987) gave values of 0.023 and 1 s^{-1} for R44L and H45Q, respectively.

Scheme IV

$$\text{ENH} \underset{k_{-1}}{\overset{k_1[H_2F]}{\rightleftharpoons}} \text{ENHH}_2\text{F} \underset{k_{-2}}{\overset{k_2}{\rightleftharpoons}} \text{ENH}_4\text{F} \underset{k_{-3}}{\overset{k_3}{\rightleftharpoons}} \text{EH}_4\text{F} \underset{k_{-4}}{\overset{k_4}{\rightleftharpoons}} \text{ENH}$$

Scheme V

$$\text{ENH} \underset{k_{-1}}{\overset{k_1[H_2F]}{\rightleftharpoons}} \text{ENHH}_2\text{F} \underset{k_{-c}}{\overset{k_c}{\rightleftharpoons}} \text{ENHH}_2\text{F}' \underset{k_{-2}}{\overset{k_2}{\rightleftharpoons}} \text{ENH}_4\text{F} \underset{k_{-3}}{\overset{k_3}{\rightleftharpoons}} \text{EH}_4\text{F} \underset{k_{-4}}{\overset{k_4}{\rightleftharpoons}} \text{ENH}$$

Relationship between k_{hyd}, V, and Product Dissociation. The pH dependencies in the steady-state parameters (V1 and V2), H_4F dissociation, and hydride transfer are illustrated in Figure 5. For H45Q, a pH dependence in the burst was observed which gives a pK_a of 7.5 ± 0.06 and a pH-independent value for k_{hyd} of 340 ± 30 s^{-1}. In contrast, for R44L, the conformational step is pH independent up to pH 9.5 (data not shown) while the hydride step shows a pK_a of 8.4 ± 0.03 and a pH-independent value for k_{hyd} of 45 ± 3 s^{-1}. For H45Q, the rate-determining step in $V2$ at low pH is the dissociation of H_4F from E–NADPH–H_4F (dashed line). This is deduced from the coincident values of 7.6 s^{-1} obtained from $V2$ (Table I) and k_{off} for the product H_4F from the ternary complex (Table IV). At pH > 9, however, hydride transfer decreases and becomes rate determining due to the ionization of the active-site proton donor Asp-27. This change in the rate-determining step is also supported by the steady-state isotope effects on V2. No pH dependence is observed in $V1$ up to 9.5 due to the relatively low value of $V1$ compared to k_{hyd} and its high pK_a (7.5). Again, the near-coincidence of $V1$ (Table I) and k_{off} for H_4F dissociation from the binary E–H_4F complex

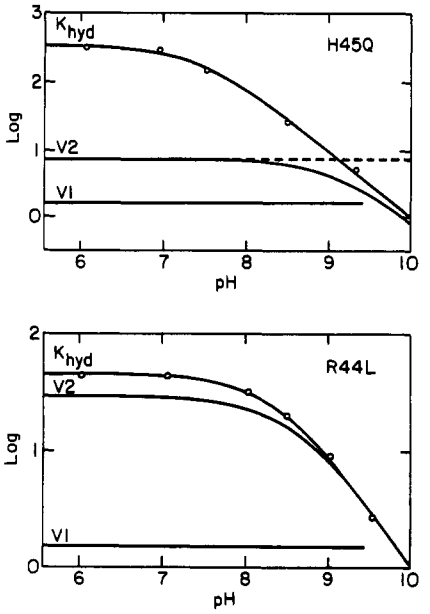

FIGURE 5: Variation of the maximal steady-state parameters, $V1$ and $V2$, and the observed hydride transfer rate, k_{hyd}, as a function of pH for H45Q and R44L at 25 °C. The solid lines for pH-dependent hydride transfer data are based on maximum rates of 340 and 45 s^{-1} for H45Q and R44L, respectively. The dashed line represents the pH-independent dissociation of H_4F from the mixed ternary complex E·NADPH·H_4F.

(Table IV) indicates that product dissociation is rate determining for $V1$. At pH > 10, hydride transfer will ultimately limit $V1$.

For R44L (Figure 5), the kinetics are more complex. Since $V2$ is only slightly lower than k_{hyd} (27 s^{-1} vs 45 s^{-1}) and a partial isotope effect is obtained at low pH, both hydride transfer and H_4F dissociation must take part in the rate limitation of $V2$ at low pH. Since $V1$ (Table I) and k_{off} for H_4F from E–H_4F (Table IV) are similar (1.7 s^{-1} vs 1.6 s^{-1}), H_4F dissociation from the binary product complex is rate determining for $V1$. In order for $V2$ to be partially limited by k_{hyd} (45 s^{-1}) the dissociation of H_4F must be accelerated in the ternary E–NADPH–H_4F complex to a rate of approximately 70 s^{-1} [$V2 = 27\ s^{-1} = 1/(1/45 + 1/70\ s^{-1})$]. This rate enhancement (70 s^{-1} vs 1.6 s^{-1}) is not observed in competition experiments, however, since the binding of NADPH to this ternary complex is sufficiently weak ($K2$ = 5000 μM). Poor signal to noise at high coenzyme concentrations prohibits measurement on a viable E·NADPH·H_4F complex. However, for both mutants, the existence of $V1$ is the result of rate-limiting H_4F dissociation from the binary E–H_4F complex. In contrast, $V2$ is the result of rate-limiting H_4F dissociation from the E–NADPH–H_4F complex for H45Q and partial limitation by both k_{hyd} and H_4F dissociation for R44L. The differences in $K1$ and $K2$ for both mutants then follow from the difference in affinities of NADPH to the binary and ternary complexes.

pH-Dependent Inhibition Studies. Stone and Morrison (1984) have shown that the pK_a of Asp-27 in the E–NADPH complex may be determined by measuring the pH-dependent dissociation constant (K_i) of the classical inhibitor 2,4-diamino-6,7-dimethylpteridine (DAM). Similar experiments performed on the two mutants show that the binary pK_a's are elevated to 7.5 ± 0.06 for H45Q and to 8.4 ± 0.1 for R44L (data not shown). Since there is no pH dependence in NADPH binding to either mutants or wild type, these pK_a's represent true values for the free enzymes. Also, since the pK_a's of the binary complex are equal to those of the ternary

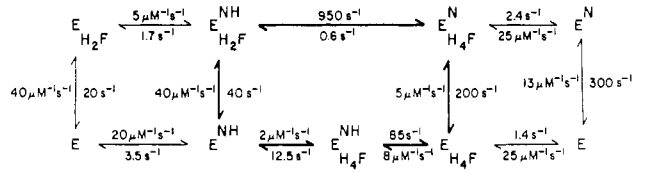

FIGURE 6: Complete, pH-independent kinetic scheme for wild-type DHFR as determined by Fierke et al. (1987) in MTEN buffer at 25 °C.

complex as measured by hydride transfer experiments, the binding of H_2F to E–NADPH must be pH independent.

Discussion

Point-site mutagenesis has become increasingly important in probing the role of individual amino acid residues at enzyme active sites (Howell et al., 1986; Fersht et al., 1988; Taira et al., 1987; Chen et al., 1985). The usefulness of this technique in understanding binding and catalysis has rested, to some part, on the assumption that the overall protein structure can tolerate a single amino acid substitution. X-ray crystallographic studies indicate that point-site mutations offer only subtle perturbations to tertiary structure and that such perturbations, if any, are accommodated by mild solvent structure reorganization (Straus et al., 1985; Clothia & Lesk, 1985). Howell et al. (1986) have solved the crystal structures of two point-site mutants of DHFR from *E. coli* (Asp-27 → Asn or Ser) and have shown that no significant changes in the backbone, side chain, or ligand conformation occur. These authors have explained the alterations in binding and catalysis by the respositioning of water molecules and the disruption of the hydrogen-bonding network around the site of mutation. In contrast, Hibler et al. (1987) have shown by two-dimensional NMR spectroscopy that substitutions at Glu-43 in the active site of staphylococcal nuclease not only affect catalysis but also produce subtle conformational changes that transmit their effects up to 30 Å from the point of mutation. To test the effects of mutations remote from the folate site of DHFR, two point-site mutations approximately 25 Å away from the active-site Asp-27 have been studied. Both mutants remove salt bridge interactions. R44L affects the interaction between the 2′-phosphate of NADPH and the guanidine side chain of R44 while H45Q affects the pyrophosphoryl linkage and the imidazole side chain of H45.

Binding Synergism. The pH-independent form of the kinetic mechanism of wild-type DHFR from *E. coli* is shown in Figure 6. An important feature of this mechanism is that NADPH binding accelerates the dissociation of H_4F from 1.4 s^{-1} in the binary E–H_4F complex to 12.5 s^{-1} in the mixed E–NADPH–H_4F ternary complex. Due to the preferred dissociation of H_4F from the ternary complex, no free enzyme is present during multiple turnovers, and the catalytic cycles are said to be "interlocked". The synergism responsible for this effect is not limited to H_4F binding but also is manifested in NADPH binding in the mixed ternary complex E–NH–H_4F. The off rate NADPH is raised from 3.5 s^{-1} in the binary E–NADPH complex to 85 s^{-1} in the ternary complex.

This synergistic effect between H_4F and NADPH is evident in the wild type and the mutants, although to varying extents. Since the binding of coenzyme can occur at two discrete points in the mechanism with different affinities, it is reasonable to expect that this phenomenon will be evident in the steady-state kinetics. For wild type, however, Lineweaver–Burk plots are virtually linear over all concentrations of NADPH (Fierke et al., 1987). Presumably, the first K_m for NADPH is very low [K_d(NADPH) = 0.33 μM] and, therefore, difficult to measure. The observed K_m (5 μM) represents mostly the binding of NADPH to E–H_4F (Fierke et al., 1987). For the mutants, however, the two K_m's can be distinguished for two reasons: (1) the binding of NADPH to the free enzymes is now sufficiently weakened (Table II); (2) in the case of R44L, H_4F loosens the binding of NADPH beyond what is seen for wild type. The binding of coenzyme to wild type is weakened from 0.2 to 10 μM in the binary E–NH and ternary E–NH–H_4F complexes, respectively (as measured by k_{off}/k_{on}, Figure 6). Assuming that $K2$ (Table I) is a close approximation to the K_d for NADPH to the ternary E–NADPH–H_4F complex for R44L, then the binding of NADPH is weakened from 3.5 μM (Table II) to 5000 μM. This means that H_4F destabilizes the binding of NADPH 2.3 kcal/mol for wild type but as much as 4.3 kcal/mol for R44L. When the same analysis for H45Q is used, NADPH binding is destabilized by only 2.2 kcal/mol. This implies that for R44L H_4F provides a more unfavorable conformation for E–NADPH than does wild type or H45Q. Also, these results suggest that Arg-44 is critical in maintaining "normal" coenzyme/product synergism while His-45 is less critical.

As H_4F affects NADPH binding in ternary complexes, the coenzyme also exerts its influence on the binding of H_4F. These effects are particularly manifest in the pH–rate profiles for the mutants (Table I and Figure 5). At sufficiently low NADPH concentrations ([NADPH] ≪ $K2$), the mixed ternary complexes for H45Q and R44L are thermodynamically inaccessible, and as a result, the rate-determining step for $V1$ follows the pH-independent dissociation of H_4F from the binary E–H_4F complexes. However, at higher NADPH levels ([NADPH] ≫ $K1$), the mixed ternary complexes may be populated so that H_4F dissociation is accelerated. As shown in Figure 5, for H45Q, this dissociation step controls $V2$ only at low pH while for R44L it is elevated above hydride transfer (k_{off} = 70 s^{-1} vs k_{hyd} = 45 s^{-1}) so that the chemical step partially controls $V2$. These increases in k_{off} for H_4F in the mixed ternary complex closely parallel the increase in dissociation constant for NADPH in the same complex. While H_4F is destabilized 1.2 kcal/mol by NADPH for the wild type (1.4 vs 12 s^{-1}; Figure 5) and 1.0 kcal/mol for H45Q (1.6 vs 7.6 s^{-1}; Table IV), it is destabilized 2.3 kcal/mol for R44L (1.6 vs 70 s^{-1}). Again, synergistic effects are augmented for R44L but not for H45Q. This is consistent with R44L being an important mutation for coenzyme/product binding control but not H45Q.

Long-Range Effects. In general, point-site mutations of DHFR have been previously considered local and structurally nondisruptive if two kinetic parameters are met: (1) changes at one binding site have no effect on the binding of ligands to the other site; and (2) the changes have no effect on the overall equilibrium between the two native conformers of the enzyme, E_1 and E_2. However, this approach excludes the detection of subtle changes that are less important either in the formation of binary complexes or in the maintenance of overall protein structure. For example, although salt bridge manipulation at the coenzyme site has no effect on H_2F binding or the equilibrium for E_1 and E_2, the free enzyme pK_a of Asp-27 (25 Å away) is raised from 6.5 in wild type to 7.5 and 8.4 in H45Q and R44L, respectively. The destabilization of Asp-27 by as much as 2.6 kcal/mol in the latter mutant clearly illustrates that single mutations can affect other residues without affecting binding or gross tertiary structure and can transmit changes over long ranges. In addition, it is reasonable to assume that these effects are due to structural and not electrostatic perturbations in the protein on the basis

of their magnitude and distance (Russell & Fersht, 1987). To illustrate this point, assume that the major effect of R44L is to remove a positive charge that is situated approximately 25 Å away from Asp-27 in the apoprotein. On the basis of the simple Coulombic calculations of Russell and Fersht (1987), a dielectric constant of 5 would be needed to support the pK_a change observed for R44L. This requires an intraprotein medium with a dielectric constant akin to that of hexane.

Although Kraut and co-workers (Filman et al., 1982) have detected no large conformational changes between E–MTX and E–MTX–NADPH complexes of *L. casei* DHFR, clearly subtle changes can occur in the E–NADPH–H_4F ternary complex for *E. coli* DHFR so that both NADPH binding and H_4F binding are equally loosened relative to their binary complexes (Figure 6). As previously shown in the steady-state, stopped-flow, and equilibrium binding experiments, although mixed ternary formation weakens the binding of the constituent ligands, the larger effects seen for R44L compared to H45Q and wild-type enzymes indicate that either greater and/or, at least, different conformational changes are occurring in this mutant. Although one interpretation of this effect may lie in the predominant importance of the 2′-phosphate/guanidine salt interaction in stabilizing the NADPH–H_4F complex, another may involve the specific nature of the replacements. R44L closely represents a complete disruption of an ionic/ionic contact by an apolar residue. H45Q, however, replaces the ionic contact with a polar/ionic interaction. Residual binding energy in the latter case due to hydrogen bonding may account for the weaker affinities of both H_4F and NADPH to the mixed ternary complex of H45Q relative to wild type. For R44L, however, there are no residual binding effects since NADH, a coenzyme analogue of NADPH lacking the 2′-phosphate, binds with equal affinity to both wild type and R44L (Table II). These results indicate that the loss in binding energy for R44L relative to wild type is due solely to the loss of a salt bridge interaction.

Ligand Binding and Isomerization. Close inspection of stopped-flow fluorescence data indicates that NADPH binding is more complex than the scheme proposed by Cayley et al. (1981). Although the coenzyme clearly binds with a fast ligand-dependent phase followed by a much slower independent one (0.03 s^{-1}), the fast phase divides into two distinguishable, ligand-dependent transients at very low and high concentrations of NADPH. These two phases can be linearly correlated (Figure 3) and ascribed to E_1 and E_2 binding. Furthermore, Blakley et al. (1988) assert that the two forms of the binary complex, E_1–NADPH and E_2–NADPH, can interconvert. Our results are in accord with their finding (Scheme II). Although there are two binary complexes, at equilibrium 99% of the enzyme is E_1–NADPH so that binding of H_2F to the E_2–NADPH complex is kinetically insignificant. Thus, Cayley's mechanism (Scheme I) is, for practical purposes, a sufficient solution although clearly a simplification.

To describe sufficiently the kinetics of NADPH binding for both mutants, it is important that the kinetic data mesh with the thermodynamic constraints of coenzyme binding. For wild-type DHFR, the overall thermodynamic dissociation constant (K_d) for NADPH can be related to the rate constants in Scheme II by eq 2 where K_i and K_i' represent the ratios of

$$K_d = \frac{K_i(1 + 1/K_{eq})}{1 + K_i/K_i'K_{eq}} \quad (2)$$

k_{off}/k_{on} and k_{off}'/k_{on}' for E_1 and E_2, respectively. By substitution of the on and off rates for E_1 and E_2 binding and the equilibrium constant K_{eq} for wild type, the K_d determined by fluorescence titration (Table II) is predicted from the stopped-flow binding data (Scheme II). Similarly, the kinetics of NADPH binding are consistent with equilibrium measurements for H45Q but not R44L. The predicted K_d for H45Q and R44L based on eq 2 is 2.6 and 60 μM, respectively. This compares with the experimental K_d of 2.0 μM for H45Q and 3.5 μM for R44L (Table II). Since the stopped-flow experiments predominantly yield information about the tight binding conformer, namely, E_1, it is unlikely that the disparity between predicted and experimental K_d's can be due to the binding of E_2 in addition to E_1. Alternatively, since a fast isotope-insensitive phase precedes the hydride step (Figure 4), it is likely that this step is associated with an altered conformation for NADPH on the enzyme. Since it has been shown that H_2F does not affect the binding of NADPH to the wild-type enzyme (Fierke et al., 1987), it appears reasonable that the isomerization step detected in catalytic turnover of the ternary complex (Scheme V) applies to the binary species as well. With this assumption, the binding mechanism can be written as in Scheme VI. Since relaxation stopped-flow binding experiments have also shown that E_2 binds NADPH very weakly for both mutants ($K_i' \approx 140$ and 340 μM for H45Q and R44L, respectively; data not shown), this step is ignored in Scheme VI. Due to large values for K_i', the denominator term in eq 2 approaches 1. If the fast isomerization step seen in the pre-steady-state experiment for R44L can be directly linked to a second ligand-independent binding step, then the rate for this isomerization, 370 ± 40 s^{-1}, should be equivalent to $k_f + k_r$. Equation 2 then can be modified to eq 3 which incorporates the isomerization, where $K_{iso} = k_f/k_r$.

$$K_d = K_i(1 + 1/K_{eq})/(1 + K_{iso}) \quad (3)$$

Thus, from substitution of data from Table III, the isomerization equilibrium constant must be large ($K_{iso} > 10$). Since the measurement of k_{on} and k_{off} by a relaxation method is influenced by a subsequent isomerization step when k_{on}[NADPH] ≤ k_f, the experimental ratio of k_{off}/k_{on} (K_i) is apparent and only sets a lower limit for the true value.[2]

The combination of binding, steady-state, and pre-steady-state data has shown that the effects of both mutants can be understood in light of the complete kinetic mechanism for wild-type DHFR (Figure 6). There are several unique points that separate the mutants from wild type and from each other: (1) Although there is only one form of the binary E–NADPH complex for both wild type and H45Q, there are two forms of the binary complex for R44L. (2) Although the binding

Scheme VI

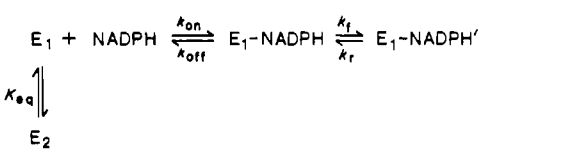

[2] For two-step binding mechanisms as in Scheme VI, kinetic simulations using KINSIM have shown that the correct assignment of k_{on} and k_{off} from binding traces is only made under limiting values of k_{on}[NADPH] and k_f. When k_{on}[NADPH] < k_f, the transients are monophasic and linearly dependent on [NADPH]. Under these conditions, the slope is the true k_{on} while the intercept underestimates the true k_{off}. When k_{on}[NADPH] ≈ k_f, the transients are biphasic although the faster phase is difficult to isolate from the second due to its low relative amplitude. Consequently, k_{obs} is a composite of two phases with the larger amplitude being associated with the isomerization step. For these cases, the slope may underestimate the true k_{on} while the intercept may overestimate the true k_{off}. When k_{on}[NADPH] > k_f, the transients are again biphasic although the faster phase is linearly dependent on [NADPH] and comprises most of the relative amplitude. Under these conditions, the slope and the intercept are the true k_{on} and k_{off}, respectively.

of NADPH is equivalently weakened in both mutants, binding of reduced folates to the free enzyme is unaffected. (3) Hydride transfer is fast for H45Q (340 s^{-1}) but slow for R44L (45 s^{-1}). (4) H_4F dissociation can occur from either the E–H_4F binary of the E–NH–H_4F ternary complexes although the latter complex is highly disfavored for R44L.

Conclusions

We have used a combination of steady-state, pre-steady-state, and binding techniques to study the kinetic behavior of two point-site mutants of DHFR, R44L and H45Q. Both mutations are located at the NADPH site and, accordingly, affect coenzyme binding. Although H_2F binding is unaffected, NADPH is loosened by 1.1 and 1.5 kcal/mol relative to wild type for H45Q and R44L, respectively. Although detailed stopped-flow binding experiments indicate that NADPH binds both enzyme conformers (E_1 and E_2) of wild type, the affinity of the coenzyme for E_1 is 100-fold greater than for E_2 so that at equilibrium only one form of the binary complex, E_1–NADPH, predominates. In contrast, pre-steady-state transients indicate that an isomerized form of bound NADPH exists for R44L which may account for the reduced rate of hydride transfer compared to H45Q and wild type [k_{hyd}(wt) = 950 s^{-1}, k_{hyd}(H45Q) = 340 s^{-1}, and k_{hyd}(R44L) = 45 s^{-1}]. In addition, the reduced hydride transfer step may reflect the influence of an increase in the intrinsic basicity of Asp-27, in the mutations that would lower the concentration of an N-5-protonated species required for reduction. This influence may predominate over the effect of the mutation on substrate or cofactor binding.

Both the acidity of Asp-27 and the stability of the mixed ternary complex, E–NH–H_4F, were found incredibly sensitive to both mutations despite their distal relationship to Asp-27 (25 Å). The pK_a was raised from 6.5 in wild type to 7.5 in H45Q and as high as 8.4 in R44L. In addition, the stability of the mixed ternary complex was lowered 2.5 kcal/mol for R44L. These effects suggest that both substrate and coenzyme sites function together and that any correlations drawn between binding and catalysis must bear this in mind.

Acknowledgments

We thank Carol A. Fierke and Kazunari Taira for help with the kinetic and equilibrium measurements. We also thank Jin-Tann Chen and Cindon Herndon for the mutant enzymes, Patricia A. Jennings for the wild-type DHFR, Carston R. Wagner for the purification of NADPD, Bruce Posner for the purification of NADPH, and Kaye Yarnell for the typing of the manuscript.

References

Barshop, B. A., Wrenn, R. F., & Frieden, C. (1983) *Anal. Biochem. 130*, 134–145.

Birdsall, B., Burgen, A. S. V., & Roberts, G. C. K. (1980) *Biochemistry 19*, 3723–3731.

Blakley, R. L. (1960) *Nature (London) 188*, 231–232.

Cayley, P. J., Dunn, S. M. J., & King, R. W. (1981) *Biochemistry 20*, 847–879.

Chen, J.-T., Mayer, R. J., Fierke, C. A., & Benkovic, S. J. (1985) *J. Cell. Biochem. 29*, 73–82.

Chen, J.-T., Taira, K., Tu, C. D., & Benkovic, S. J. (1987) *Biochemistry 26*, 4093–4100.

Chothia, C., & Lesk, A. M. (1985) *J. Mol. Biol. 182*, 151–158.

Curthoys, H. P., Scott, J. M., & Rabinowitz, J. C. (1972) *J. Biol. Chem. 247*, 1959–1964.

Dawson, R. M. C., Elliott, D. C., Elliott, W. H., & Jones, K. M. (1969) in *Data for Biochemical Research*, Oxford University Press, Oxford, U.K.

Dunn, S. M. J., Batchelor, J. G., & King, R. W. (1978) *Biochemistry 17*, 2356–2364.

Dunn, S. M. J., & King, R. W. (1980) *Biochemistry 19*, 766–773.

Dyson, R. D., & Isenberg, I. (1971) *Biochemistry 10*, 3233–3241.

Fersht, A. R., Leatherbarrow, R. J., & Wells, T. N. C. (1987) *Biochemistry 26*, 6030–6038.

Fierke, C. A., Johnson, K. A., & Benkovic, S. J. (1987) *Biochemistry 26*, 4085–4092.

Filman, D. J., Bolin, J. T., Matthews, D. A., & Kraut, J. (1982) *J. Biol. Chem. 257*, 13663–13672.

Hibler, D. W., Stolowich, N. J., Reynolds, M. A., Gerlt, J. A., Wilde, J. A., & Bolton, P. H. (1987) *Biochemistry 26*, 6278–6286.

Howell, E. E., Villafranca, J. E., Warren, M. S., Oatley, S. J., & Kraut, J. (1986) *Science (Washington, D.C.) 231*, 1123–1128.

Howell, E. E., Warren, M. S., Booth, C. L. J., Villafranca, J. E., & Kraut, J. (1987) *Biochemistry 26*, 8581–8598.

Johnson, K. A. (1986) *Methods Enzymol. 134*, 677–705.

Kallen, R. G., & Jencks, W. P. (1966) *J. Biol. Chem. 241*, 5845–5850.

Mathews, C. K., & Huennekens, F. M. (1960) *J. Biol. Chem. 235*, 3304–3308.

Penner, M. H., & Frieden, C. (1985) *J. Biol. Chem. 260*, 5366–5369.

Perry, K. M., Onuffer, J. J., Touchette, N. A., Herndon, C. S., Gittleman, M. S., Matthews, C. R., Chen, J.-T., Mayer, R. J., Taira, K., Benkovic, S. J., Howell, E. E., & Kraut, J. (1987) *Biochemistry 26*, 2674–2682.

P-L Biochemicals (1961) Circular OR-18, P-L Biochemicals, Milwaukee, WI.

Rabinowitz, J. C. (1960) *Enzymes, 2nd Ed. 2*, 185–252.

Russel, A. J., & Fersht, A. R. (1987) *Nature (London) 328*, 496–500.

Seeger, D. R., Cosulick, D. B., Smith, J. M., & Hultquist, M. E. (1949) *J. Am. Chem. Soc. 71*, 1753–1758.

Segel, I. H. (1975) in *Enzymes Kinetics, Behavior and Analysis of Rapid Equilibrium and Steady-State Enzyme Systems*, p 109, Wiley, New York.

Stone, S. R., & Morrison, J. F. (1982) *Biochemistry 21*, 3757–3765.

Stone, S. R., & Morrison, J. F. (1984) *Biochemistry 23*, 2753–2758.

Straus, D., Kawashima, R. E., Knowles, J. R., & Gilbert, W. (1985) *Proc. Natl. Acad. Sci. U.S.A. 82*, 2272–2276.

Taira, K., & Benkovic, S. J. (1988) *J. Med. Chem. 31*, 129–137.

Viola, R. E., Cooke, P. F., & Cleland, W. W. (1979) *Anal. Biochem. 96*, 334–340.